PCCP

Accepted Manuscript


This is an *Accepted Manuscript*, which has been through the Royal Society of Chemistry peer review process and has been accepted for publication.

*Accepted Manuscripts* are published online shortly after acceptance, before technical editing, formatting and proof reading. Using this free service, authors can make their results available to the community, in citable form, before we publish the edited article. We will replace this *Accepted Manuscript* with the edited and formatted *Advance Article* as soon as it is available.

You can find more information about *Accepted Manuscripts* in the Information for Authors.

Please note that technical editing may introduce minor changes to the text and/or graphics, which may alter content. The journal's standard Terms & Conditions and the Ethical guidelines still apply. In no event shall the Royal Society of Chemistry be held responsible for any errors or omissions in this *Accepted Manuscript* or any consequences arising from the use of any information it contains.

ROYAL SOCIETY OF CHEMISTRY

www.rsc.org/pccp

Journal Name

RSCPublishing

ARTICLE

# $TiO_2$ nanotubes sensitized with CdSe via RF Magnetron Sputtering for photoelectrochemical applications under visible light irradiation

Cite this: DOI: 10.1039/x0xx00000x

Received 00th January 2012,
Accepted 00th January 2012

DOI: 10.1039/x0xx00000x

www.rsc.org/

Jesum A. Fernandes,[a] Pedro Migowski,[b] Zacarias Fabrim,[b] Adriano F. Feil,[c] Guilherme Rosa,[b] Sherdil Khan,[b] Guilherme J. Machado,[b] Paulo F.P. Fichtner,[d] Sérgio R. Teixera,[b] Marcos J. L. Santos[a] and Jairton Dupont[a,*]

Highly ordered $TiO_2$ NT arrays were easily decorated with CdSe via RF magnetron sputtering. After deposition thermal annealing at different temperatures was performed to obtain an improved $TiO_2$/CdSe interface. The heterostructures were characterized by RBS, SEM, XRD, HRTEM, UV-Vis, EIS, IPCE and current *versus* voltage curves. The sensitized semiconducting electrodes display enhanced photocurrent density of ca. 2 $mA.cm^{-2}$ at 0.6 V (vs Ag/AgCl) under visible light ($\lambda$>400 nm). The sensitized photoelectrodes displayed 3 and 535 times fold enhanced photocurrent when compared to bare $TiO_2$ NTs under 1 sun and under visible light illumination, respectively. IES results confirmed the improved charge transfer across the $TiO_2$/CdSe/electrolyte interface after annealing at 400ºC. Incident photon-to-electron conversion efficiency measurements confirmed the efficient sensitization by allowing photoresponse in the visible range.

## 1. Introduction

Due to the growing demand for energy, worldwide research has been focused on the study and development of new and efficient ways to obtain renewable energy. Among all the alternatives, hydrogen is one of the most promising candidates due to its environmental friendly and renewable aspects.[1,2] Moreover, producing hydrogen using solar irradiation by photoelectrochemical (PEC) water splitting have been attracting large interest since this process can diminish green house gases emission due to the input of light energy.[3-5] Regarding this technology, highly ordered $TiO_2$ nanotube arrays have been applied as photoanode in photoelectrochemical cells due to its high chemical stability in aqueous media, associated with large surface area, high conductivity and relatively low production cost.[6,7] Nevertheless, due to the wide band gap (~ 3.2 for anatase) $TiO_2$ absorbs only UV light which limits the efficiency for direct solar energy conversion. Different approaches have been explored to improve light absorption of $TiO_2$, as for instance doping to create donor and acceptor levels within the band gap.[8-11] Another promising way is developing heterostructures, using low band gap sensitizers such as CdSe, CdS and CdTe, which allows for photoexcited electron transfer to the conduction band of $TiO_2$. These sensitizers are usually obtained by colloidal synthesis, spray pyrolysis and chemical bath deposition.[7,12-17] On the other hand, physical vapour deposition (PVD) techniques are currently widely used in large-scale thin film photovoltaic (PV) devices manufacturing. Furthermore, the most efficient and lower cost per watt 2nd generation PV cells are produced by PVD techniques such as sputtering deposition.[18-21] Within this context, developing new methodologies can contribute to the understanding of the $TiO_2$/sensitizer interface and therefore to the development of efficient photoelectrochemical devices. Curiously, the scientific literature lacks reports on the use of sputter deposition of II-VI semiconductors for the $TiO_2$ sensitization. Thus, considering the high efficiencies obtained in PV technologies and the easy up scaling, one might expect that by using sputtering deposition, highly efficient photoelectrodes can be produced.

In this work, we report the use of radio-frequency (RF) magnetron sputtering to sensitize $TiO_2$ NTs with CdSe nanoparticles and the study of the influence of CdSe concentration and thermal annealing on the photoelectrochemical and electrical properties of the heterostructures.

## 2. Experimental

### 2.1 Synthesis of $TiO_2$ NTs

$TiO_2$ NTs were prepared by anodization process, carried out in a standard two-electrode electrochemical cell with platinum foil as counter electrode, under constant applied voltage of 20 V during 1 h, in ultrasonic bath. The electrolyte solution was 0.5 wt% $NH_4F$, 10 wt% $H_2O$ and ethylene glycol. The as-anodized samples were annealed at 400°C for 3h with ramping rate of 5ºC.$min^{-1}$ under air.[6,22-24]

### 2.2 CdSe deposition by RF Sputtering

CdSe was deposited on $TiO_2$ NTs substrate, by the technique of RF magnetron sputtering using a compost target of CdSe (99.999%). The background sputtering pressure was $2x10^{-9}$ mbar and the

Physical Chemistry Chemical Physics Accepted Manuscript

working pressure was $2x10^{-2}$ mbar under Ar (99.9999%). A 5 min pre-sputtering was performed to clean the CdSe target before deposition. The sputtering was carried out with RF power of 50 W and deposition rate of 0.057 $nm.s^{-1}$ at 25 °C, during different periods of 5, 30 and 60 min. After deposition, the samples were annealed at different temperatures 300°C, 400°C and 500°C under vacuum ($2x10^{-7}$mbar) for 30 minutes.

### 2.3 Composition, morphology, optical and structural characterizations

Rutherford backscattering spectrometry (RBS) analysis were carried out using $He^{++}$ ions beam. The detector was positioned at 15° from the beam. Fig. 1a shows the RBS spectrum obtained with beam energy of 1.4 MeV and Figs. 1b and 4a with beam energy of 3 MeV. The morphologies of pristine $TiO_2$ NTs and the heterostructures were characterized by scanning electron microscopy (SEM) in a JEOL 6060. Glancing angle XRD measurements were carried out using a Philips diffractometer with $K_\alpha$ radiation ($\lambda$ = 1:54 Å). All the measurements were performed with lower angle incidence of 2 ° and angular step of 0.02 ° for every 20 s intervals within the angular region $2\theta$ = 20 ° - 50 °. The phases were identified by the software Crystallographica Search Match together with the database ICSD - PDF2-International Centre for Diffraction Data. The samples were investigated by high resolution transmission electron microscopy (HRTEM) using a JEM2010 operated at 200 kV and a TITAN microscope operated at 300 kV. The atomic positions were observed by high-angle annular dark field (HAADF) scanning transmission electron microscopy (STEM) images and energy dispersive x-ray spectroscopy (EDS) line profiles, performed in a Titan microscope operated at 300 kV. The samples were prepared by dispersing a few milligrams of freestanding CdSe/$TiO_2$ NTs in acetone at room temperature and drop casting the solution on a 400 mesh carbon-coated Cu grid. UV-vis diffuse reflection was performed by spectrophotometry Varian Cary 5000 UV-Visible.

### 2.4 Photoelectrochemical characterization

Photocurrent-voltage (*I-V*) and electrochemical impedance spectroscopy (EIS) experiments were carry out using an Autolab model PGSTAT 100N. The experiments were performed in a quartz cell using standard three-electrode configuration, a platinum wire was used as counter electrode, Ag/AgCl as reference and CdSe/$TiO_2$ NTs as working electrode.

During photocurrent-voltage measurements the working electrode was irradiated with a 300 W Xenon lamp. For polychromatic irradiation the light intensity was calibrated to 100 $mW.cm^{-2}$ and either AM 1.5G filter (1 sun) or UV cut-off filter (visible light, $\lambda \geq 400$ nm) were used. The electrolyte was 0.24 M $Na_2S$ and 0.35 M $Na_2SO_3$ aqueous solution, used to prevent photocorrosion of the CdSe.[25,26]

The EIS measurements were performed under dark conditions with frequency range from 100 kHz to 0.1 Hz and amplitude of 10 mV under open circuit voltage.[27-29]

Incident photon-to-electron conversion efficiency (IPCE) measurements were performed in a keithley 2400 SourceMeter and a monochromator cornerstone Oriel. A coiled platinum wire in a two electrode cell was used as counter electrode.[30-32]

## 3. Results and discussion

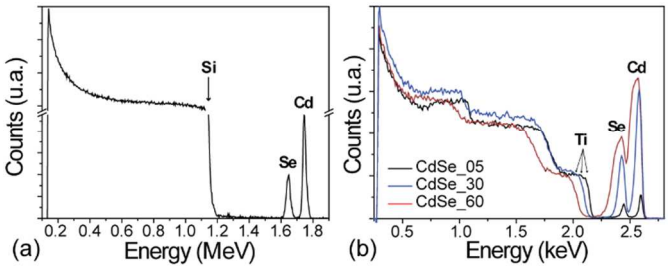


**Fig. 1.** RBS spectra of CdSe on silicon substrate obtained after 1 minute deposition (a), and CdSe on $TiO_2$ NTs obtained after 05 min, 30 min and 60 min deposition(b).

In order to isolate the CdSe from the $TiO_2$ and from impurities related to the anodization process, we have obtained the RBS spectrum of pure CdSe on silicon (Si) substrate (Fig. 1a). One can observe the presence of Si, Cd and Se clearly showing the formation of a highly pure material presenting a 1:1 stoichiometry.[33,34] For the CdSe deposited on $TiO_2$ NTs (Fig.1b) the 1:1 stoichiometric is also observed, however for shorter deposition periods there is a small deficiency of Cd (see Table 1).

The SEM images of the as-deposited samples shows that the top tubes coverage becomes thicker as the CdSe target is sputtered for longer periods (Fig.2a). STEM analyses were used to evaluate the CdSe distribution on the outer/inner wall of $TiO_2$ NTs (Fig.2b and c). Although CdSe was deposited on all length of the tubes, the highest concentration is localized on the top of the NTs (Fig. 2b). It is possible to observe that CdSe deposition follow the nanotubes template without blocking it. This result corroborates the SEM images from CdSe_30. Fig. 2c shows the CdSe clusters distribution on the outer and inner wall of the $TiO_2$ NTs. In addition, EDS spectra (Fig. 2d) confirm the presence of CdSe on the edge and the centre of the nanotubes. The increase in sputtering time also results in spectral absorption broadening through the visible range (Fig. 3a). The samples obtained after 30 and 60 min of deposition absorb in nearly the entire visible spectrum, meanwhile the sample obtained after 5 minutes present about the same

**Table 1.** Characteristics of $TiO_2$/CdSe photoanodes produced by RF magnetron sputtering.

| Samples | Deposition time (min) | Annealing (°C) | Concentration ($x10^{17}$ at.$cm^{-2}$) | | Rate |
|---|---|---|---|---|---|
| | | | Cd | Se | Cd/Se |
| CdSe_05 | 05 | - | 0.54 | 0.55 | 0.98 |
| CdSe_30 | 30 | - | 3.18 | 3.21 | 0.99 |
| CdSe_60 | 60 | - | 6.37 | 6.40 | 1.00 |
| CdSe_30/300 | 30 | 300 | 2.99 | 3.03 | 0.99 |
| CdSe_30/400 | 30 | 400 | 2.90 | 2.95 | 0.98 |
| CdSe_30/500 | 30 | 500 | <LOQ | <LOQ | <LOQ |
| LOQ: Limit of quantification | | | | | |

Physical Chemistry Chemical Physics Accepted Manuscript


This journal is © The Royal Society of Chemistry 2012

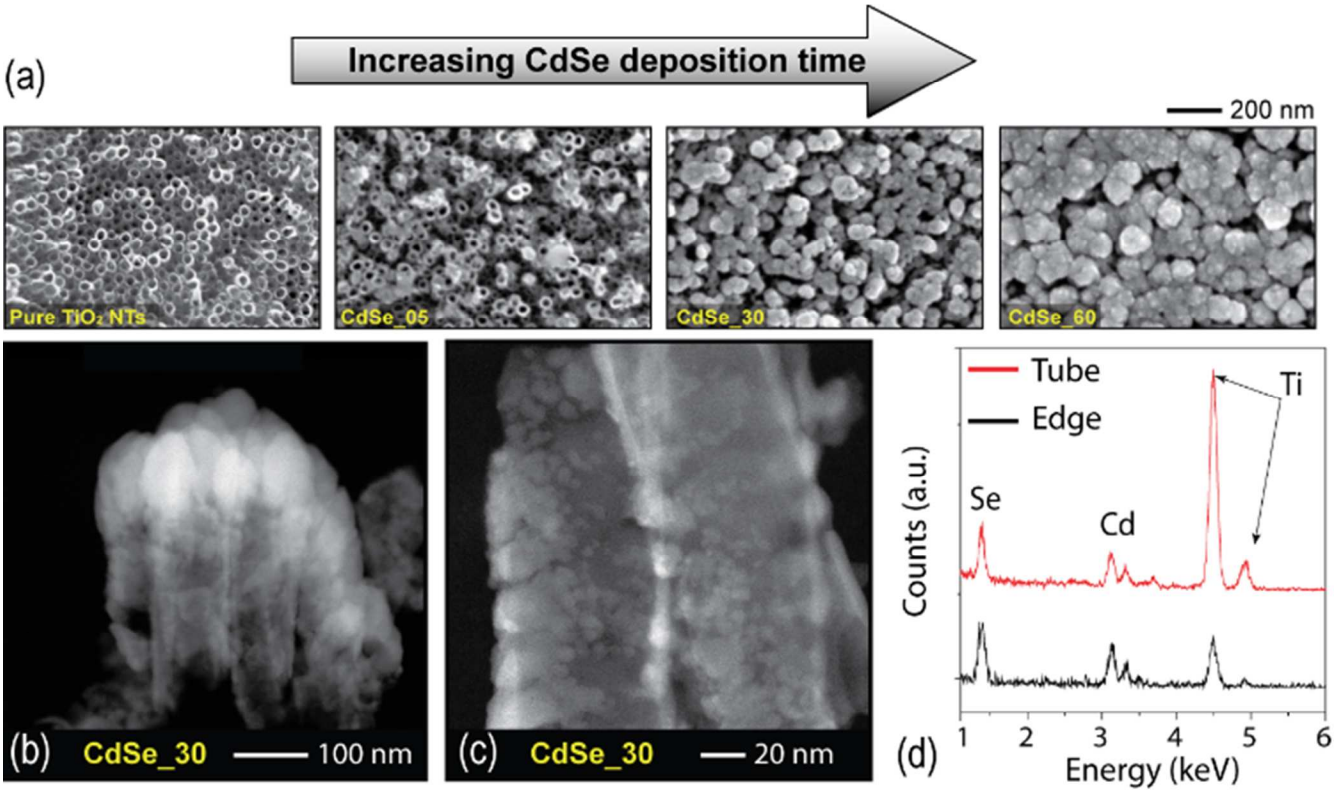


**Fig. 2.** SEM images of samples obtained with different deposition times (a) STEM images showing CdSe distribution on the $TiO_2$ NTS for sample CdSe_30 (b, c) and EDS of sample CdSe_30 to confirm presence of CdSe. (d).

spectrum that pure $TiO_2$. The maximum absorbance for CdSe_30 and CdSe_60 are observed at 500 nm and 550 nm, respectively, indicating an increase in average crystal size of CdSe. The absorption band observed for pure $TiO_2$ from *ca.* 400 to *ca.* 600 nm is characteristic of highly-ordered titania nanotube arrays on Titanium foil. Studies on the propagation of electromagnetic waves in the ultraviolet-visible range through these samples have shown that a gradient in the oxide composition from the top of the barrier layer to the Ti metal, result in absorption bands in the visible range.[35]

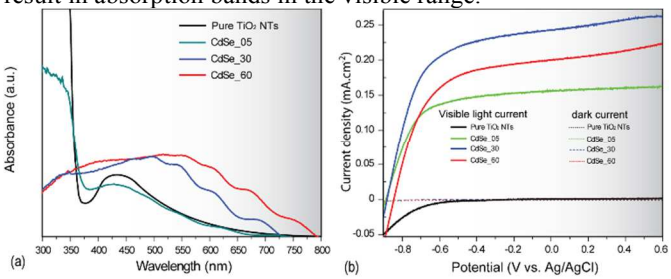


**Fig. 3** UV-vis spectra obtained by diffuse reflection mode (a) and photoelectrochemical measures presented current density-voltage characteristics using visible light irradiation (b)

Current density *versus* potential (*J x V*) curves, obtained under visible-light show an interesting relation between optical and photoelectrochemical properties of the $TiO_2$/CdSe heterostructures (Fig. 3b). The open circuit potential ($V_{oc}$) of the sensitized samples shifted to more negative potentials, to around – 1.0 V *vs* Ag/AgCl, in relation to the pure $TiO_2$ sample ($V_{oc}$ of – 0.85 V). In addition, all samples showed anodic currents upon illumination, indicating the n-type nature of the semiconductor electrodes. As expected, due to the very low absorptivity under visible irradiation the photocurrent density (*J*) of pure $TiO_2$ NTs resembled those exhibited under dark conditions. On the other hand, the CdSe sensitized samples showed PEC response under visible light conditions. Among the sensitized samples, the CdSe_05 which presented the lowest absorbance under visible light, Fig. 3a, also generated the lowest photocurrent Fig. 3b. In addition, the best PEC response was obtained from CdSe_30 and not from CdSe_60, although the last presents the highest absorbance under visible spectrum.

These results strongly suggest that although increasing CdSe thickness improves optical absorption it also decreases the electron transfer yield from the CdSe sensitizer to the $TiO_2$.

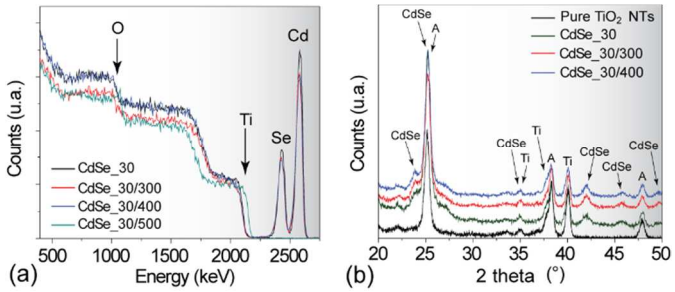


Fig.4. RBS spectra after annealing (a), structural characterization by XRD (b)

Physical Chemistry Chemical Physics Accepted Manuscript

It is well established that proper annealing can improve particles interaction, thus PEC performance of semiconductor heterostructures.[1,36]

Therefore CdSe_30 samples were annealed at 300, 400 and 500°C aiming to enhance current density responses. RBS analyses showed that thermal annealing process does not considerably affect the stoichiometry of the samples, although for the samples CdSe_30/300 and CdSe_30/400 a 6 % and 9 % loss of CdSe was observed. However, as observed by RBS the CdSe layer vanished completely from the sample CdSe_30/500 (Table 1 and Fig. 4a). Fig. 4b shows the XRD patterns of the samples. The characteristic peak of $TiO_2$ has been identified at 25.4° which is related to the anatase phase. This peak is observed for all samples, however it broadened when compared to pure $TiO_2$ due to the overlapping of CdSe hexagonal phase. The peaks characteristic of CdSe observed at 23.8, 42, 45.8 and 49.7° have no interference from the $TiO_2$ NTs substrate. According to SEM and UV-vis analyses before and after annealing the morphology and the optical properties of these samples are not dependent on the thermal treatment. Fig. 5 shows HRTEM images of CdSe crystals covering $TiO_2$ NTs corroborating with STEM analyses.

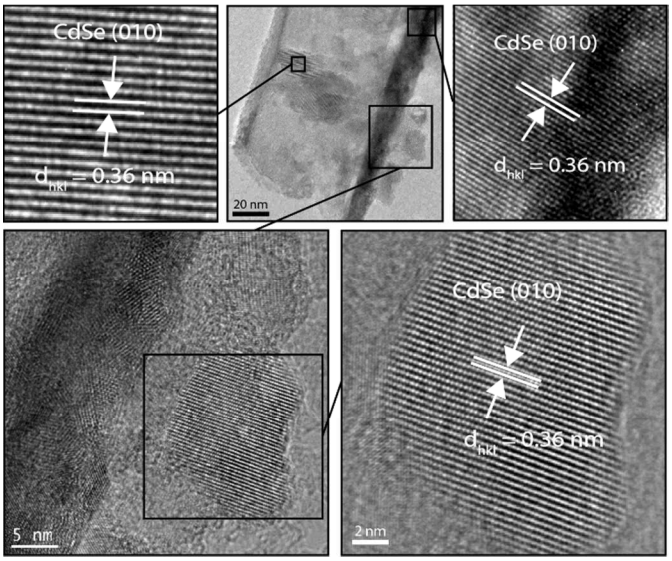


**Fig. 5** HRTEM image showing the lattices fringes of CdSe for sample CdSe_30/400.

The image shows a detailed view of the HRTEM contrast and the distances of the patterns in good agreement with {010} planes of CdSe present in hexagonal phase, which corroborates the XRD results.

In order to evaluate the effect of post deposition thermal treatment on the PEC performance of CdSe_30, *J x V* curves were obtained under both 1 sun and visible light irradiations, Fig. 6a-b.

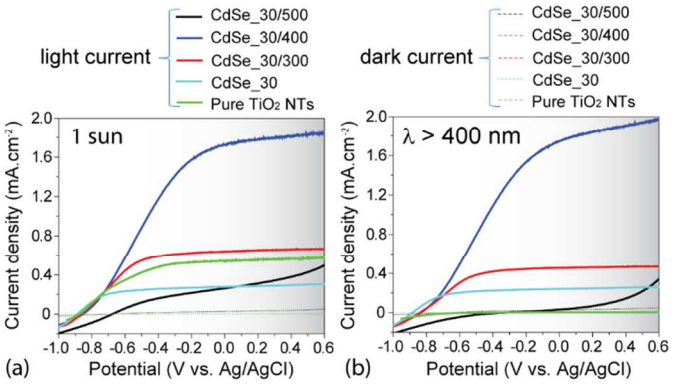


**Fig. 6.** Current versus potential curves for samples with different annealing, measured under 1 sun irradiation (a) and visible light irradiation(b).

Under AM 1.5G conditions, pure $TiO_2$ NTs present efficiency similar to other systems using the same electrolyte. The worst PEC behaviour was obtained from the sample CdSe_30/500 since the *JxV* measurements reveals very low photocurrent in addition to a not squared curve expected for an efficient system, Fig.6a. These results were already expected once according to the RBS spectrum, the CdSe was completely removed from the substrate after annealing at 500 °C. Another interesting result is that although sensitized with CdSe, under 1 sun irradiation the CdSe_30/300 generated nearly the same current densities than pure $TiO_2$ NTs (Fig.6a). On the other hand, CdSe_30/400 presented a 3 times fold enhancement photocurrent when compared to pure $TiO_2$, at 0.6 V *vs* Ag/AgCl, resulting in a maximum photocurrent value of ~ 1.8 $mA.cm^{-2}$. The results obtained under visible light are shown in Fig.6b. As expected, no photocurrent was generated from pure $TiO_2$ NT as it poorly absorb in the visible range. In addition, samples CdSe_30/300 and CdSe_30/400 presented similar photocurrents to those under 1 sun. One can observe a 1.5 and 7 times photocurrent enhancement from samples CdSe_30/300 and CdSe_30/400 respectively, when compared to CdSe_30 (Fig. 6a, b).

These results clearly indicate the existence of an optimum annealing temperature, creating a synergistic interaction between the two materials, improving PEC performance. The improved interaction at the $TiO_2$/CdSe interface should result in decreased charge transfer resistance and enhanced photocurrent. To elucidate the underlying mechanism of post annealing related to the interface charge transfer, EIS was performed for the samples CdSe_30 and CdSe_30/400. Fig 7a shows the Nyquist plots obtained for samples CdSe_30 and CdSe_30/400 characteristic of heterogeneous systems. High frequency response represents trapping/detrapping of electrons or electrolyte/counter electrode interface charge transfer. The plots of Fig 7b represents the cutoff frequency for this charge process which is almost 90 Hz. Similarly, low frequency response conveys the valence band charge transfer resistance at the semiconductor/electrolyte interface.

Physical Chemistry Chemical Physics Accepted Manuscript


This journal is © The Royal Society of Chemistry 2012

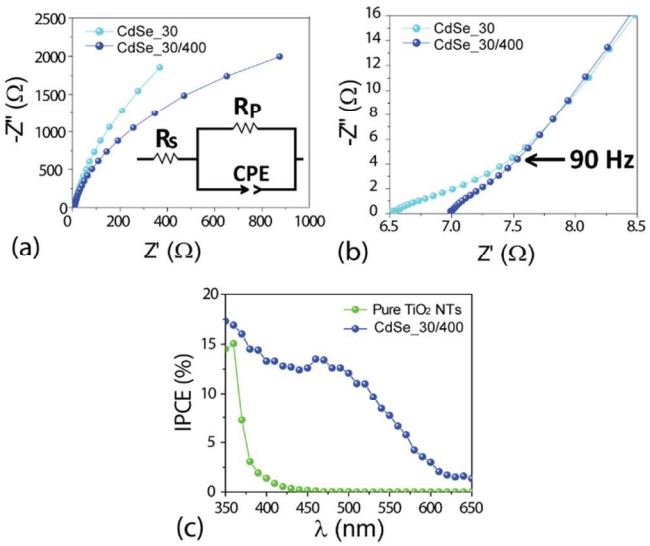


**Fig. 7.** The EIS measurement to verify annealed effect in charge transfer (a) show with details high frequency to samples CdSe_30 and CdSe_30/400 (b) IPCE analyses of de $TiO_2$ NTs pure and the sample CdSe present highest photocurrent(c)

The arc obtained for CdSe_30/400 clearly indicates low charge transfer resistance when compared to CdSe_30. Considering the Nyquist plots one can observe the existence of only one time constant, resulting from the formation of a CdSe layer deposited by RF magnetron sputtering covering the $TiO_2$ surface. This result is interesting, once the literature reports two times constants for systems sensitized by chemical routes.[37-39] The total charge transfer resistance at the $TiO_2$/CdSe interface was calculated by fitting the EIS spectrum considering a series resistance (Rs) with a CPE parallel to resistor (Rp). The series resistance was found to be 7.3 Ω for both samples, which corroborates the Fig 7b at 90 Hz giving nearly the same resistance. The parallel resistance was calculated to be 6 kΩ for CdSe_30/400 and 17 kΩ for CdSe_30. Similarly the Voc under dark for CdSe_30 was measured as -0.43 V whereas for CdSe_30/400, it was -0.55 V (Vs Ag/AgCl). The charge transfer resistance values and the open circuit voltage clearly shows that CdSe_30/400 presents improved charge transfer properties when compared to CdSe_30, which corroborates the photocurrent-voltage measurements (Fig 6a and 6b).

Figure 7c shows the IPCE results for pristine $TiO_2$ nanotubes and for the CdSe_30/400. Pristine $TiO_2$ presents strong photoresponse in the near-UV region, however a dramatic drop of IPCE is observed for wavelength >370 nm. This result is already expected by considering the large band gap o pure $TiO_2$.

**Table 2.** EIS results to samples as deposited and annealed.

| Samples | $R_S$ (Ω) | $R_p$ (kΩ) | CPE (μF) | n | Voc (v) |
|---|---|---|---|---|---|
| CdSe_30 | 7.28 | 17.05 | 810 | 0.95 | -0.42 |
| CdSe_30/400 | 7.30 | 6.01 | 650 | 0.96 | -0.57 |

The sensitized nanotubes (CdSe_30/400) present the ability to harvest and convert light to current in a broad wavelength range, from the near-UV region until around 650 nm. These results are in agreement with the UV-vis spectra (Figure 3a) showing a match between the optical and the photoelectrochemical behavior of the heterostructure. The IPCE results clearly shows that RF magnetron sputtering can be efficiently used to sensitize $TiO_2$ nanotubes, improving light absorption, in addition to allow photogenerated electrons transfer from the CdSe to $TiO_2$, increasing IPCE. According to the photoelectrochemical measurements, CdSe main role is absorbing visible light and generating excited electrons, while $TiO_2$ major role is allowing charge carriers conduction towards the collecting electrode. This result is interesting, once the literature using either 1 sun[1,7] or visible light[13,14] obtain different results, suggesting that $TiO_2$ absorption plays an important role on the obtained photocurrent.

## 4. Conclusions

In summary, $TiO_2$ NTs are efficiently sensitized with CdSe using RF magnetron sputtering technique, resulting in visible light active heterostructure photoanode. Charge transfer across $TiO_2$/CdSe interface as well as photocurrent generation can be improved by controlling annealing temperature. The best photoelectrochemical response was obtained from CdSe_30/400, presenting photocurrent density of 1.9 $mA.cm^{-2}$ at 0.6 V vs Ag/AgCl, resulting in 3 and 535 times enhancement when compared to pure $TiO_2$ NTs under 1 sun and visible light irradiation. Finally this approach can lead to a more efficient and clean technique to obtain heterostructures with application on different photoelectrochemical devices, including solar cells.

## Acknowledgements

The authors thank CNPq, CAPES, GEPSI-PUCRS, Nanolab-UFRGS, Laboratório de Implantação Iônica-UFRGS, Laboratório de Óptica-UFRGS, Centro de Microscopia Eletrônica-UFRGS and to Prof. Dr. Daniel L. Baptista for the use TITAN localized in IMETRO.

## Notes and references

[a]Universidade Federal do Rio Grande do Sul, Instituto de Química, Av. Bento Goncalves, 9500, P.O.Box 15003, CEP 91501-970, Porto Alegre, RS, Brazil. Email: jairton.dupont@ufrgs.br
[b]Universidade Federal do Rio Grande do Sul, Instituto de Física, Av. Bento Goncalves, 9500, 91501-970, Porto Alegre, RS, Brazil.
[c]Pontificia Universidade Católica do Rio Grande do Sul, Faculdade de Física, Av. Ipiranga, 6681, 90619-900, Porto Alegre, RS, Brazil.
[d]Universidade Federal do Rio Grande do Sul, Escola de Engenharia, Av. Bento Goncalves, 9500, 91501-970, Porto Alegre, RS, Brazil.

† Electronic Supplementary Information (ESI) available:

See DOI: 10.1039/b000000x/

(1) Ai, G.; Sun, W.; Gao, X.; Zhang, Y.; Peng, L.-M. *Journal of Materials Chemistry* **2011**, *21*, 8749.
(2) Mor, G. K.; Varghese, O. K.; Wilke, R. H. T.; Sharma, S.; Shankar, K.; Latempa, T. J.; Choi, K.-S.; Grimes, C. A. *Nano Letters* **2008**, *8*, 1906.

Physical Chemistry Chemical Physics Accepted Manuscript

(3) Fujishima, A.; Honda, K. *Nature* **1972**, *238*, 37.
(4) Zhang, Y.; Schnepp, Z.; Cao, J.; Ouyang, S.; Li, Y.; Ye, J.; Liu, S. *Sci. Rep.* **2013**, *3*.
(5) Paracchino, A.; Laporte, V.; Sivula, K.; Grätzel, M.; Thimsen, E. *Nat Mater* **2011**, *10*, 456.
(6) Jun, Y.; Park, J. H.; Kang, M. G. *Chemical Communications* **2012**, *48*, 6456.
(7) Gao, X.-F.; Sun, W.-T.; Ai, G.; Peng, L.-M. *Applied Physics Letters* **2010**, *96*.
(8) Asahi, R.; Morikawa, T.; Ohwaki, T.; Aoki, K.; Taga, Y. *Science* **2001**, *293*, 269.
(9) Xu, M.; Da, P.; Wu, H.; Zhao, D.; Zheng, G. *Nano Letters* **2012**, *12*, 1503.
(10) Park, J. H.; Kim, S.; Bard, A. J. *Nano Letters* **2005**, *6*, 24.
(11) Mohapatra, S. K.; Misra, M.; Mahajan, V. K.; Raja, K. S. *The Journal of Physical Chemistry C* **2007**, *111*, 8677.
(12) Shin, K.; Seok, S. i.; Im, S. H.; Park, J. H. *Chemical Communications* **2010**, *46*, 2385.
(13) Chouhan, N.; Yeh, C. L.; Hu, S.-F.; Liu, R.-S.; Chang, W.-S.; Chen, K.-H. *Chemical Communications* **2011**, *47*, 3493.
(14) Yang, H.; Fan, W.; Vaneski, A.; Susha, A. S.; Teoh, W. Y.; Rogach, A. L. *Advanced Functional Materials* **2012**, *22*, 2821.
(15) Mukherjee, B.; Smith, Y. R.; Subramanian, V. *The Journal of Physical Chemistry C* **2012**, *116*, 15175.
(16) Su, F.; Lu, J.; Tian, Y.; Ma, X.; Gong, J. *Physical Chemistry Chemical Physics* **2013**, *15*, 12026.
(17) Mukherjee, B.; Wilson, W.; Subramanian, V. *Nanoscale* **2013**, *5*, 269.
(18) Bosio, A.; Romeo, A.; Menossi, D.; Mazzamuto, S.; Romeo, N. *Crystal Research and Technology* **2011**, *46*, 857.
(19) Repins, I.; Contreras, M. A.; Egaas, B.; DeHart, C.; Scharf, J.; Perkins, C. L.; To, B.; Noufi, R. *Progress in Photovoltaics: Research and Applications* **2008**, *16*, 235.
(20) Wada, T.; Kohara, N.; Nishiwaki, S.; Negami, T. *Thin Solid Films* **2001**, *387*, 118.
(21) Paudel, N. R.; Yan, Y. *Thin Solid Films* **2013**, *549*, 30.
(22) Alivov, Y.; Fan, Z. Y.; Johnstone, D. *Journal of Applied Physics* **2009**, *106*.
(23) Macak, J. M.; Tsuchiya, H.; Ghicov, A.; Yasuda, K.; Hahn, R.; Bauer, S.; Schmuki, P. *Current Opinion in Solid State and Materials Science* **2007**, *11*, 3.
(24) Rani, S.; Roy, S. C.; Paulose, M.; Varghese, O. K.; Mor, G. K.; Kim, S.; Yoriya, S.; LaTempa, T. J.; Grimes, C. A. *Physical Chemistry Chemical Physics* **2010**, *12*, 2780.
(25) Buehler, N.; Meier, K.; Reber, J. F. *The Journal of Physical Chemistry* **1984**, *88*, 3261.
(26) Hensel, J.; Wang, G.; Li, Y.; Zhang, J. Z. *Nano Letters* **2010**, *10*, 478.
(27) Jung, M.-H.; Kang, M. G. *Journal of Materials Chemistry* **2011**, *21*, 2694.
(28) Kim, K. K., M.-J.; Kim, S.-I.; Jang, J.-H. *Sci. Rep.* **2013**, *3*.
(29) Bertoluzzi, L.; Bisquert, J. *The Journal of Physical Chemistry Letters* **2012**, *3*, 2517.
(30) Guijarro, N.; Lana-Villarreal, T.; Mora-Seró, I.; Bisquert, J.; Gómez, R. *The Journal of Physical Chemistry C* **2009**, *113*, 4208.
(31) Yan, J.; Ye, Q.; Zhou, F. *RSC Advances* **2012**, *2*, 3978.
(32) Yum, J.-H.; Baranoff, E.; Wenger, S.; Nazeeruddin, M. K.; Gratzel, M. *Energy & Environmental Science* **2011**, *4*, 842.
(33) Chu, W. K. M., J. W.; Nicolet, M.A. *Backscattering Spectroscopy*; Academic Press: New York, 1978.
(34) Behar, M.; Fichtner, P. F. P.; Grande, P. L.; Zawislak, F. C. *Materials Science and Engineering: R: Reports* **1995**, *15*, 1.
(35) Grimes, C. A., Mor, Gopal K. *TiO2 Nanotubes Arrays - Synthesis, Properties and Applications*; Springer US: Springer US, 2009.
(36) C. F. Chi, S. Y. L. a. Y. L. L. *Nanotechnology* **2010**, *21*.
(37) Johansson, V.; Ellis-Gibbings, L.; Clarke, T.; Gorlov, M.; Andersson, G. G.; Kloo, L. *Physical Chemistry Chemical Physics* **2014**, *16*, 711.
(38) Jun, H.; Careem, M.; Arof, A. *Nanoscale Research Letters* **2014**, *9*, 69.
(39) Mane, R. S.; Shinde, D. V.; Joon Yoon, S.; Ambade, S. B.; Kee Lee, J.; Han, S.-H. *Applied Physics Letters* **2012**, *101*.

Physical Chemistry Chemical Physics Accepted Manuscript


This journal is © The Royal Society of Chemistry 2012

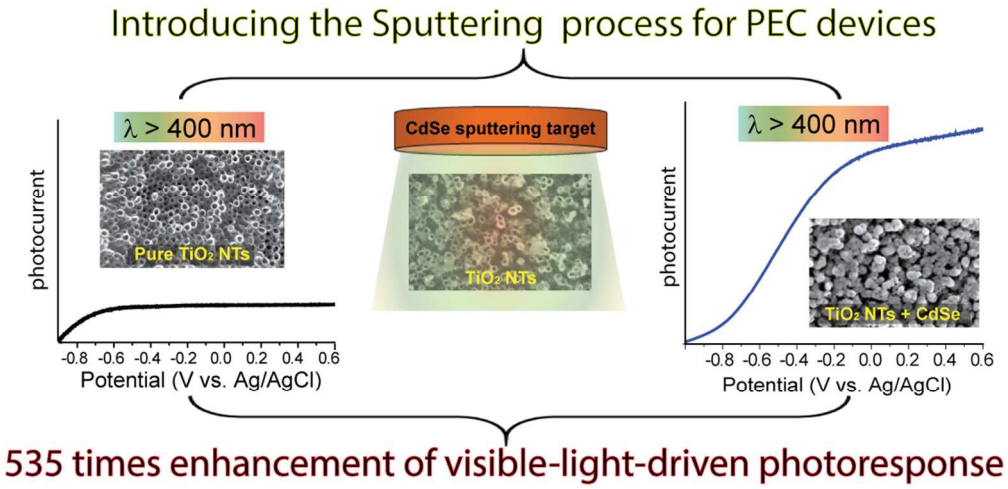


100x48mm (300 x 300 DPI)

Physical Chemistry Chemical Physics Accepted Manuscript